Available online at www.sciencedirect.com
SCIENCE DIRECT®
Journal of Theoretical Biology 231 (2004) 357–376
Journal of Theoretical Biology
www.elsevier.com/locate/yjtbi

Identifying control mechanisms of granuloma formation during *M. tuberculosis* infection using an agent-based model

Jose L. Segovia-Juarez[1], Suman Ganguli[1], Denise Kirschner*

Department of Microbiology and Immunology, University of Michigan, Ann Arbor, MI 48109, USA

Received 14 April 2004; received in revised form 28 June 2004; accepted 30 June 2004
Available online 26 August 2004

Abstract

Infection with *Mycobacterium tuberculosis* is a major world health problem. An estimated 2 billion people are presently infected and the disease causes approximately 3 million deaths per year. After bacteria are inhaled into the lung, a complex immune response is triggered leading to the formation of multicellular structures termed granulomas. It is believed that the collection of host granulomas either contain bacteria resulting in a latent infection or are unable to do so, leading to active disease. Thus, understanding granuloma formation and function is essential for improving both diagnosis and treatment of tuberculosis. Granuloma formation is a complex spatio–temporal system involving interactions of bacteria, specific immune cells, including macrophages, CD4+ and CD8+ T cells, as well as immune effectors such as chemokine and cytokines. To study this complex dynamical system we have developed an agent-based model of granuloma formation in the lung. This model combines continuous representations of chemokines with discrete agent representations of macrophages and T cells in a cellular automata-like environment. Our results indicate that key host elements involved in granuloma formation are chemokine diffusion, prevention of macrophage overcrowding within the granuloma, arrival time, location and number of T cells within the granuloma, and an overall host ability to activate macrophages. Interestingly, a key bacterial factor is its intracellular growth rate, whereby slow growth actually facilitates survival.

Keywords: Granuloma formation; Tuberculosis; Agent based model; *Mycobacterium tuberculosis*

1. Introduction

Tuberculosis (TB) is the world's leading cause of death due to infectious disease. There are approximately 8 million new cases of the disease annually, resulting in an estimated 2–3 million deaths per year. Even more remarkable, it is estimated that one-third of the world population is infected with *Mycobacterium tuberculosis* (Mtb), the causative agent of the disease (World Health Organization, 2001).

This large discrepancy between the number of infected individuals (on the order of billions) and the numbers of annual cases resulting in death (on the order of millions) points to an important fact about tuberculosis. Most individuals infected with *M. tuberculosis* do not progress to active disease. It is believed that only 5–10% of infected individuals develop active disease within 2 years of initial infection (Comstock, 1982; Styblo, 1980). The vast majority are able to contain infection but not clear it, achieving *latent* tuberculosis through mounting a successful adaptive immune response. Although most individuals are able to maintain latency, they are at risk of developing active TB by reactivation, which occurs at a rate of 5–10% during their lifetime. It is thought that reactivation occurs when the immune system is compromised in some way, such

*Corresponding author. Tel.: +1-734-647-7722; fax: +1-734-647-7723.
E-mail addresses: jlsj@umich.edu (J.L. Segovia-Juarez), sganguli@itsa.ucsf.edu (S. Ganguli), kirschne@umich.edu (D. Kirschner).
[1]Co-first authors with equal contribution—no order is implied.

0022-5193/$ - see front matter © 2004 Elsevier Ltd. All rights reserved.
doi:10.1016/j.jtbi.2004.06.031

as due to co-infection with HIV, abuse of alcohol or drugs, or simply waning immunity due to aging. Exogenous reinfection may also occur (Singer and Kirschner, 2004).

The adaptive immune response to *M. tuberculosis* results in the formation of characteristic multicellular structures within lung tissue of infected individuals called granulomas. The formation and maintenance of these granulomas likely plays a central role in the pathogenesis of the disease. It is conjectured that small, solid granulomas contain infection and do not induce significant pathology, whereas large, necrotic granulomas may lead to bacterial dissemination and greater pathology (Saunders and Cooper, 2000). Thus, an understanding of granuloma formation and function is essential to understanding host–pathogen interactions during infection with *M. tuberculosis*, and ultimately toward treatment and prevention.

The adaptive immune response, however, is a complex process involving spatial and temporal organization and interactions of numerous elements: bacteria, chemokines, cytokines, adhesion molecules, and immune effector cells. Particularly in humans, few data exist characterizing the process of granuloma formation and function, and only recently have non-human primate models been developed to begin to study this system in vivo (Capuano et al., 2003). The complexity of the adaptive immune response to *M. tuberculosis*, which we describe in detail in Section 2, indicates that mathematical and computational models may be a key means to further understanding this system (Perelson, 2002). Towards this goal, we have developed an agent-based model of the adaptive, spatio–temporal immune response to *M. tuberculosis*.

Wigginton and Kirschner (2001) did initial work in this direction by developing a model to examine temporal dynamics of the host adaptive immune response to *M. tuberculosis* infection. Their model consisted of a system of nonlinear ordinary differential equations that sought to capture key interactions between various populations of bacteria, macrophages, T cells and cytokines. Marino and Kirschner (2004) and Marino et al. (2004) extended this work to a two-compartment ODE model to study trafficking of dendritic cells and T cells between the lung and lymph node. Two other papers from our group introduced models for examining spatial aspects of the adaptive immune response to *M. tuberculosis* infection within the lung and specifically the process of granuloma formation. Gammack et al. (2003) developed a partial differential equations model of the innate immune response to Mtb infection and the early stages of granuloma formation. Ganguli et al. (submitted) used a metapopulation framework, in which ordinary differential equations represented spatially distinct cellular subpopulations within a discretized spatial domain.

Differential equations have been the most widely applied formalism for mathematical and computational modeling of biological systems. Another formalism that has more recently been developed and applied to study complex systems are agent-based models (ABMs). ABMs grew out of research in cellular automata and artificial life. The defining feature of agent-based models is that elements of the system are represented primarily as discrete agents with several unique attributes. Individual agents reside in an explicitly represented spatial environment. They interact with one another and with the environment according to sets of rules. Typically these rules are defined such that all interactions occur locally (with respect to the environment). Moreover, the formulation of the rules are often stochastic in nature. This is in contrast to the differential equations framework in which populations are represented by continuous variables, are assumed to be roughly homogeneous and interact deterministically.

In an agent-based model, the local, possibly stochastic, individual-level interactions give rise to global, system-wide dynamics and patterns. Thus, ABMs are particularly useful for studying complex systems in which individual heterogeneity and spatial interactions are important. For those reasons, we believe the agent-based approach is appropriate for modeling the immune response to *M. tuberculosis* and the process of granuloma formation. More generally, we believe that agent-based modeling may be appropriate for modeling many aspects of the immune system.

Agent-based models are a natural extension of cellular automata. Cellular automata have been applied to modeling a wide variety of biological systems (see Ermentrout and Edelstein-Keshet, 1993 for an excellent overview), including some aspects of the immune system (Celada and Seiden, 1992; Seiden and Celada, 1992), tumor growth (Alarcon et al., 2001; Kansal et al., 2000a,b; Qi et al., 1993; Smolle, 1998; Smolle and Stettner, 1993), and angiogenesis (Anderson and Chaplain, 1998; Markus et al., 1999). Agent-based modeling is a natural extension of cellular automata modeling, in which more complex notions can be easily formulated and implemented via object-oriented programming. To date, however, ABMs has been applied most prominently within the social sciences, going back to the early work of Schelling (Schelling, 1969, 1978) and extending to the more recent work of Axelrod (1997) and Epstein and Axtell (1996). Within biology, the approach has been applied within the fields of ecology (where it is often called individual-based modeling (Grimm, 1999)), and bacterial colony growth and biofilms (Kreft et al., 19, 2001). Mansury et al. (2002) and Mansury and Deisboeck (2003) develop and explore an agent-based model of tumor growth. Most relevant to our work here are perhaps the following papers that use ABMs to study aspects of the immune

response at the cellular level: An (2001), who presents an agent-based model of inflammation with an aim of explicating systemic inflammatory response syndrome, and Edelstein-Keshet and Spiros (2002) who develop a model of Alzheimer's Disease plaque formation.

The goal of this work is to identify control mechanisms that are important for proper granuloma formation during infection with Mtb in humans. In this work this is measured by the ability to control bacterial levels. We formulate and implement an ABM based on a minimal set of rules that qualitatively reproduces granuloma formation corresponding to distinct pathological and bacterial observed outcomes. These rules are based on known or hypothesized mechanisms involved in the immune response to Mtb infection. We describe briefly the immune response to Mtb, as well give details of the agent-based model, its rules, and the adaptation of sensitivity and uncertainty analyses for use in this setting. We describe our result in two main settings of containment and dissemination.

2. Adaptive immune response to *M. tuberculosis*

In this section, we briefly outline the current knowledge of *M. tuberculosis* (Mtb) infection and immunity. We focus on adaptive immunity, specifically on interactions between bacteria, macrophages, and T cells. These elements and their interactions form the basis of our agent-based model, which we present in the following section. We discuss what is known and/or conjectured about how these interactions contribute to granuloma formation, and how granulomas may contribute to latency.

M. tuberculosis is a rod bacteria, approximately 2–5 μm long and 0.2–0.3 μm thick. It is non-motile gram-positive (Grosset et al., 2000) and is aerosol-transmitted. Exposed individuals typically inhale droplets containing bacteria. Droplets may reach lung alveloae where they encounter resident macrophages. Macrophages phagocytose bacteria that they may kill, resulting in clearance of initial infection via innate immunity (Dannenberg and Rook, 1994). In their "resting" (i.e., inactivated) state, however, these resident macrophages are less efficient at killing bacteria than macrophages that have been activated for the task. Moreover, *M. tuberculosis* has evolved mechanisms for evading killing by its host macrophages (McDonough et al., 1993). Thus, it is much more likely that resting resident macrophages are unable to clear the bacteria they phagocytose, in which case they become "infected" macrophages.

Mycobacteria replicate well within infected macrophages. *M. tuberculosis* prefer the intracellular environment, and replicate at a faster rate than they do extracellularly (Zhang et al., 1998). Infected macrophages may burst due to an excessive number of intracellular bacteria. This releases formerly intracellular bacteria into the extracellular environment, inducing a new round of macrophage infections, contributing to infection spread.

Although individuals will most likely not clear infection in such cases, the host immune system can *contain* infection by mounting an adequate adaptive immune response. Infected macrophages release cytokines and chemokines that attract dendritic cells and additional macrophages (Orme and Cooper, 1999; Sadek et al., 1998). Other cells such as PMNs and mast cells also secrete chemokines, but for this study we only consider macrophages known to participate in the granuloma response (Seiler et al., 2003). Dendritic cells engulf bacteria and then migrate to the nearest draining lymph node where they present antigen to naive T cells. This induces differentiation and activation of T cells that subsequently migrate back to the lung and to specific sites of infection, likely guided by adhesion molecules and chemokine signals produced by infected macrophages (Saunders and Cooper, 2000; Tufariello et al., 2003).

Both CD4+ and CD8+ T cells participate in the immune response. Activated T cells of both types contribute to control of infection by activating macrophages (via production of cytokines such as IFN-γ) and by lysing chronically infected macrophages (via apoptosis and cytotoxic T cell action) (Flynn and Chan, 2001; Flynn and Ernst, 2000). Activated macrophages are highly efficient at phagocytosing and eliminating extracellular bacteria, while lysis of chronically infected macrophages serves to release *M. tuberculosis*, allowing their uptake by activated macrophages. This migration of macrophages, T cells and other immune cells to the site of infection and their subsequent interactions result in the formation of granulomas. These structures are spherical accumulations with a characteristic spatial pattern, consisting of the various cell types discussed above (bacteria, macrophages, T cells), as well as other types of immune cells (such as natural killer cells, PMNs and B cells) (Dannenberg and Rook, 1994; Seiler et al., 2003). Fig. 1 shows two histological sections of granulomas from a non-human primate model of Mtb infection. Panel A shows an outcome of a solid granuloma containing infection, while in contrast panel B shows a disseminated (caseous) granuloma where bacteria and necrotic tissue spreads. The diameter of both granulomas shown in Panels A and B is 2 mm.

Granulomas are thought to be the means by which the adaptive immune response achieves and maintains latency in tuberculosis. The structure of a functioning granuloma physically contains infection: the accumulation of immune cells around the local site of infection likely prevents its dissemination. Moreover, it has also been conjectured that the spatial structure of granulomas provide a framework for effective localized

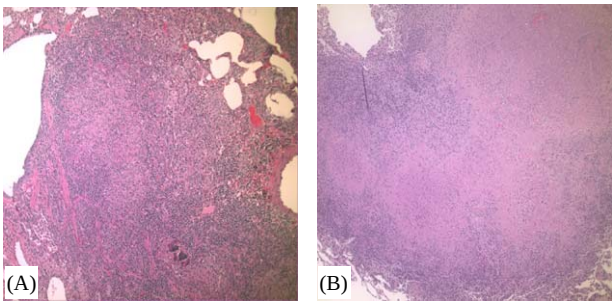

Fig. 1. Histopathologic comparison of solid (A) and caseous (disseminated) (B) pulmonary granulomas in the lungs of *M. tuberculosis*-infected cynomolgus macaques. Solid granulomas (A) consist of a densely populated collection of inflammatory cells that include centrally located macrophages and histiocytes with surrounding rings of T cells. Caseous granulomas (B) are characterized by a central area of necrotic material, an outer later of macrophages, histiocytes and giant cells ringed by T cells. Hemotoxylin and eosin stain, total magnification 100 × . Both granulomas shown are 2 mm × 2 mm in size. (Photos donated by Dr. P. Ling Lin, in the Flynn Laboratory at the University of Pittsburgh).

interaction of the elements of adaptive immunity (Saunders and Cooper, 2000).

In the following section we present an agent-based model of adaptive immunity to *M. tuberculosis* infection. Our model is motivated by the biology discussed above and focuses on the process of granuloma formation. The environment of the model represents a two-dimensional cross-section of alveolar lung tissue where infection and granuloma formation occur. The elements of the model represent key factors involved in the processes of infection, adaptive immunity, and granuloma formation: bacteria, chemokines, macrophages, and T cells. The rules of the model represent the biological interactions described above: infection of macrophages following phagocytosis of bacteria; release of chemokines by infected macrophages; recruitment and migration of macrophages and T cells in response to chemokine signals; intracellular bacterial replication within infected macrophages, possibly leading to bursting of the host macrophage; activation and/or lysis of infected macrophages by T cells; and phagocytosis and clearance of extracellular bacteria by activated macrophages.

3. Model description and methods

The model has the following components:

(1) The *environment* where entities reside, representing a section of alveolar tissue.
(2) The *entities* of the model, consisting of discrete macrophage and T cell agents, and continuous chemokine and bacteria variables.
(3) The *rules* that govern the dynamics of the system, representing the biological interactions of the entities.
(4) The *time-scales* on which the rules are executed.

We elaborate on each of these components below.

3.1. The environment

As described in the previous section, humans are infected by *M. tuberculosis* after inhaling bacteria into the alveolar space of the lung. The majority of infections remain isolated at focal sites of infection in the lung (pulmonary tuberculosis) where granuloma formation initially occurs, and do not spread to other organs (Tufariello et al., 2003). Hence, the spatial environment of our model represents a portion of alveolar lung tissue. Specifically, the environment consists of a two-dimensional $N \times N$ lattice of *micro-compartments*. In order to avoid boundary effects, opposite edges of the lattice are identified so that the lattice is actually a torus. Model results are not constrained by this assumption, since the lattice is made large enough to contain the relevant phenomena entirely within its interior (see below).

The size of each micro-compartment is defined to contain approximately the largest cell type in our model: the alveolar macrophage. The diameter of human alveolar macrophages has been measured to be approximately 20 μm (Krombach et al., 1997). Hence, we take each micro-compartment in the lattice to represent a square with dimensions 20 μm × 20 μm. Each micro-compartment can simultaneously hold at most one macrophage, one T cell, chemokine and bacteria. This is reasonable since extracellular bacteria and chemokine molecules are orders of magnitude smaller than macrophages.

Bacterial dissemination and rapid progression to disease have been associated with larger necrotic granulomas of diameter 2 mm or more. This has been observed in both humans (Dannenberg and Rook, 1994) and more recently in non-human primates (Capuano et al., 2003)—(see for example, Fig. 1). On the other hand, containment of disease has been associated with smaller solid granulomas of diameter 2 mm and less, as observed in non-human primates infected with *M. tuberculosis* (Capuano et al., 2003). These animals showed no clinical signs of disease and had presumably contained infection.

Since we intend to simulate the formation of a single granuloma within the spatial domain of the model, we define the lattice to be large enough to contain a larger necrotic granuloma of the type associated with rapid progression to active disease. Thus, a square spatial domain of dimensions 2 mm × 2 mm suffices for

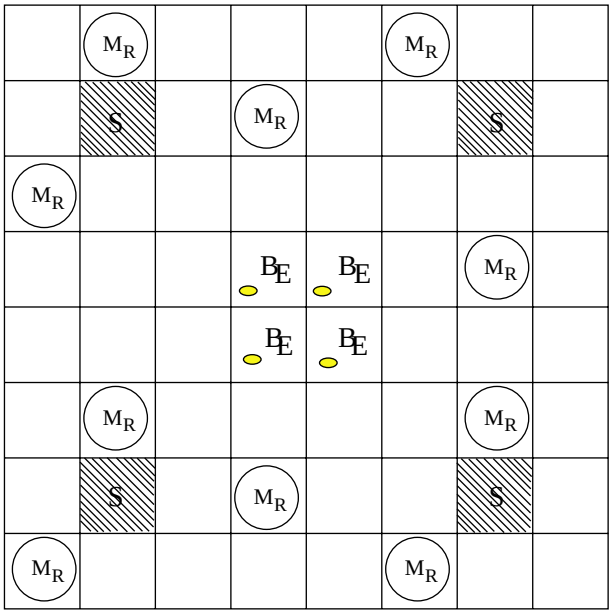

Fig. 2. The two-dimensional alveolar tissue environment is represented by a $N \times N$ lattice of micro-compartments measuring 2 mm × 2 mm. Certain micro-compartments are designated as blood vessel sources (S). Shown here are the initial conditions, where the initial load of (extracellular) bacteria (B_E) is placed at the center, and a background level of resting macrophages (M_R) is located at random locations.

our purposes, corresponding to a value of $N = 100$.[2] The results are not constrained by the size of the lattice.

A certain number of micro-compartments on the lattice are designated as *source compartments*. They represent locations where blood vessels enter the lung tissue through which new macrophages and T cells arrive at the infection site (see Section 3.3).

Fig. 2 depicts the spatial environment, including source compartments. The diagram indicates the initial state of the system: an initial innoculum of extracellular bacteria is introduced into a small number of micro-compartments near the center of the lattice, and resting macrophages are randomly distributed across the lattice. Macrophages and extracellular bacteria are among the entities of the model discussed below in Section 3.3. The initial conditions are discussed in more detail in Section 4.1.

3.2. Time

Time is discrete in this model. Thus, a simulation consists of finite *time-steps*. Each time-step corresponds to approximately 6 s of "real time". This was determined by considering the fastest process represented in the model, which is the diffusion of chemokine, calculated as described in Section 3.3.1.

The state of the system at time-step $t + 1$ is computed by applying a series of *rules* to the system at time-step t. However, most rules are executed at slower timescales than chemokine diffusion. These processes are the movement and interactions of T cells and macrophages, and are described below in Sections 3.3.3 and 3.3.4.

Rules for macrophages and T cells are updated every 10 min of real time (i.e., every 100 time-steps). This value was chosen by considering what we take to be the next fastest process, movement of T cells.

To determine how often T cell movement should be updated, we used the results of (Miller et al., 2003). By using laser microscopy for high-resolution imaging of T cells within the lymph nodes of mice, it was estimated that T cells move with an average velocity of 11 μm/min, i.e., approximately 10^{-5} m/min. It is to be expected that their velocity will be considerably slower in lung tissue. For the purposes of this paper we have assumed T cells move approximately a full order of magnitude slower. Hence, it takes 10 min for a T cell to move from a given micro-compartment to a neighboring micro-compartment in the model (T_{sp}).

Of course, actual velocities of T cells in lung tissue likely vary over a wide range depending on states of individual T cells and local environments in which they are moving. Similarly, the frequency with which all other rules are executed could vary depending on the state of the entities involved. Future refinements of this model could include more detailed and heterogeneous treatments of time such as these.

The rate of macrophage movement was calculated from the data of Webb et al. (1996), based on cloned macrophage mouse cell line BAC1.25F. They found macrophage velocities in the range of 0.12–0.5 μm/min using a Dunn chemotaxis chamber. We set the speeds to 1, and 0.0007 μm/min for resting (M_{rsp}), and infected macrophages (M_{isp}) respectively. For activated macrophages (M_{asp}) we use a range of values between 0.0125 and 1 μm/min. Simulations are performed for 200 days and up to 500 days. The typical time frame for development of a granuloma is anywhere from 14 to 100 days in non-human primates (Capuano et al., 2003 and J. Flynn, personal communication). We simulate this time frame for formation of a granuloma and also allow for an extended simulation to track long-term dynamics occurring in an infection that spans the lifetime of the host. We discuss results of both simulation time-frames below.

3.3. Entities of the system and their rules

There are four types of entities in the model: a generic chemokine, extracellular bacteria, T cells, and macrophages. Chemokine and extracellular bacteria are

[2]To make the total length of each side of the lattice 2 mm = 2×10^{-3} m (where each micro-compartment has sides of length 20 μm = 2×10^{-5}) requires 2×10^{-3} m/(2×10^{-5} m) = 100 micro-compartments/side.

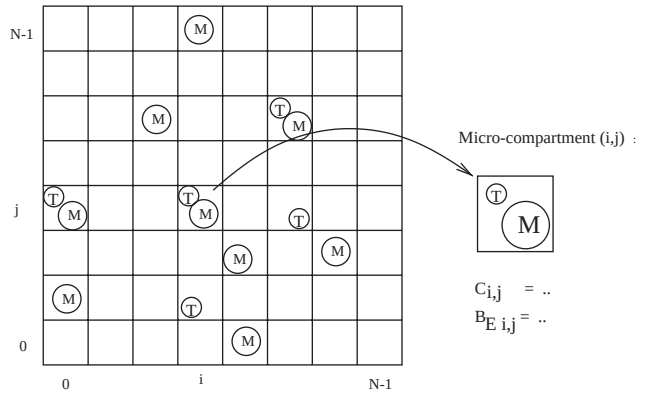

Fig. 3. A typical state of the system during infection, consisting of an $N \times N$ lattice of micro-compartments populated with discrete macrophage and T cell agents. Micro-compartment (i,j), for example, contains one macrophage agent, chemokine value $C_{i,j}(t)$, and extracellular bacteria level, $B_{Ei,j}(t)$.

treated as continuous variables that take on real values in each micro-compartment of the lattice at each time-step, whereas macrophages and T cells are represented as discrete agents. Fig. 3 depicts these entities on the lattice.

3.3.1. Chemokine

Various molecules released by macrophages and other cells acts as chemoattractants, attracting other cells to the site of infection. Chemokines perform different roles at different times during granuloma development (Lukacs and Chensue, 1996). In this work, we represent chemokines as attractors for macrophages and T cells. For this initial implementation we have chosen to represent the multiple chemokines involved in the immune response to *M. tuberculosis* infection by a composite chemokine value. We treat this chemokine concentration as a continuous variable. Thus, chemokines are represented in our model by a concentration value $C_{i,j}$ in each micro-compartment (i,j). Chemokines create a field where macrophages and T cells move toward higher concentrations. In this setting, a larger lattice (i.e. the torus) does not affect the dynamics of T cells, macrophages, or the overall infection outcome.

Chemokine molecules are very small in comparison with macrophages, so we assume that they can co-reside in a micro-compartment with macrophages. Sources of chemokine are derived from infected, chronically infected and activated macrophages (Scott et al., 2003). Chemokine is secreted from these sources and then diffuses and decays over time. Chemokine diffusion is implemented with the following rule: in each micro-compartment (i,j) the chemokine concentration $C_{i,j}$ diffuses to and from the four micro-compartments in its immediate (von Neumann) neighborhood. For readability we abbreviate the subscripts of the four neighbors by N, E, S, W, and we suppress the "(t)" notation on the chemokine variables on the right-hand side:

$$C_{i,j}(t+1) = C_{i,j} * (1-\lambda) + \lambda * (C_N + C_E + C_S + C_W)/4.$$

Here λ is a diffusion constant. Intuitively, λ measures the proportion of $C_{i,j}$ that diffuses out of micro-compartment (i,j) during each time-step. We calculate a value for λ from $\lambda = 4\delta_c \Delta t/\Delta x$, (see Ermentrout and Edelstein-Keshet, 1993), where δ_c is the diffusion constant for chemokine molecules in the diffusion PDE, Δx is the scale of the spatial discretization, and Δt is the scale of the time discretization. The values of the latter two in our model are $\Delta t = 0.1$ min and $\Delta x = 10^{-5}$ m, respectively. Values of 10^{-6} to 10^{-7} have been reported as diffusion constants for chemokine molecules (Francis and Palsson, 1997). Using a value of $\delta_c = 10^{-7}$, we obtain a value of $\lambda = 0.6$. In our analyses, for the diffusion constant λ, we use a range of values between 0.5 and 0.8.

We include a decay process in the model for chemokine. At each time-step, a certain proportion δ decays:

$$C_{i,j}(t+1) = C_{i,j} - \delta * C_{i,j}.$$

Values of 2–4 h have been reported for the half-life for the chemokine IL-8, which is centrally involved in the immune response to *M. tuberculosis* (Walz et al., 1996). Using a half-life of 2 h, we obtain a value of $\delta = 0.000577$. In our analyses, for the chemokine degradation coefficient δ, we use a range of values between 0.000288 and 0.0011.

3.3.2. Extracellular bacteria

The minimal infectious dose for *M. tuberculosis* is on the order of 10 bacteria (Capuano et al., 2003). To simulate initial infection in which a droplet containing bacteria arrives in the lung alveoli, our initial conditions include a small number of bacteria divided over a few micro-compartments near the center of the lattice, as indicated in Fig. 2. We choose the center of the lattice for easy visualization. Initial conditions are discussed in detail in Section 4.1.

Extracellular bacteria (B_E) replicate rather slowly; reports of *M. tuberculosis* in lung tissue of mice have estimated an extracellular doubling time of 62 h (North and Izzo, 1993). For simplicity, we use a doubling time of 75 h. This yields a discretized growth rate of $\alpha_{BE} = 0.00015/\text{min}$ in the following rule for extracellular bacterial replication. We also assume an upper bound of $K_{BE} = 200$ bacteria (10 times the number of bacteria that an infected macrophage can contain before bursting) within each micro-compartment, and that extracellular bacterial replication follows logistic growth with

respect to this upper bound:

$$B_E(t+1) = B_E(t) + \alpha_{BE} * B_E(t) * (1 - (B_E(t)/(K_{BE} * 1.1))).$$

We consider extracellular bacteria diffusion to be a slow process that we do not presently include, however the model can easily incorporate this process.

3.3.3. T cells

T cells are represented as discrete agents that can enter and reside on the lattice. Up to one T cell can share a micro-compartment with a macrophage. T cells have only *age* and *position* attributes. At day 10 of infection (T_{delay}), T cells enter the lattice with a probability T_{recr}, via source micro-compartments in response to chemokine level at those locations (we explore this delay in greater detail below). This captures recruitment of immune cells to the site of infection in response to chemotactic signals. New T cells are assigned a lifespan (T_{ls}) randomly selected between 0 and 3 days (Sprent, 1993). The age of each T cell is incremented at each time-step. A T cell is removed from the lattice when its age reaches its lifespan, representing natural death.

Movement of T cells is affected by the local chemokine gradient on the lattice, and T cells can only recognize chemokine values of $C_{i,j} > 1$. Movement of each T cell is a biased random walk with probabilities calculated as a function of the chemokine concentrations of the eight neighboring micro-compartments around the T cell. If the chosen target location is empty, then the T cell moves to the target micro-compartment. If the chosen target location is occupied by another T cell, then the T cell remains stationary. If the target location does not contain a T cell but is occupied by a macrophage, then the T cell moves to the target micro-compartment with a given small probability (T_{move}). In this way we capture any crowding effects imposed by macrophages on T-cell movement.

Activated T cells are immune effector cells that perform two important functions: they activate infected macrophages and they kill chronically infected macrophages. In our model, we combine the effects of CD4+ T cell and CD8+ T cells into a composite T cell population. These distinct classes of T cells perform different cytotoxic functions, leading to death of infected macrophages. These functions are implemented in the model according to rules described in the next section.

3.3.4. Macrophages

Macrophages are represented as discrete agents that reside on the lattice. At most one macrophage can occupy a given micro-compartment. Macrophages have the following attributes:

- Position.
- Age.

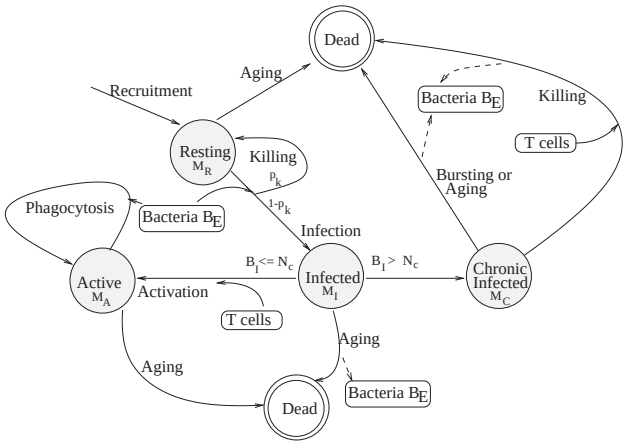

Fig. 4. Macrophage state diagram. Circles are macrophage states and arrows represent processes; these are described in detail in Section 3.3.4. A macrophage dies when it reaches its lifespan. B_E is the number of extracellular bacteria, and p_k is the probability of killing by resting macrophage of extracellular bacteria. Resting macrophages (M_R) become infected by bacteria (with probability $1-p_k$) or can kill (with probability p_k). Infected macrophages (M_I) with intracellular bacterial load (B_I) less than N_c can be activated by T cells. If B_I is greater than N_c the macrophage becomes chronically infected (M_C). T cells activate macrophages (M_A) which can then phagocytose and eliminate extracellular bacteria. A chronically infected macrophage (M_C) bursts if its intracellular bacterial load (B_I) is greater than the macrophage carrying capacity (K_{BI}). Chronically infected macrophages can be killed by a T cell located in the same micro-compartment.

- Number of intracellular bacteria (B_I), a non-negative integer such that $0 \leqslant B_I < K_{BI}$, where K_{BI} is a parameter representing the average intracellular bacterial carrying capacity of macrophages.[3]
- State, defined from one of the following 4 states: resting (M_R), infected (M_I), chronically infected (M_C), or activated (M_A) (see Fig. 4).

Like T cells, new (resting) macrophages enter the lattice with a probability M_{recr}, via the source micro-compartments in response to the chemokine level at those locations (represented by "Recruitment" in Fig. 4). Specifically, if micro-compartment (i,j) is a source and the amount of chemokine $C_{i,j}$ exceeds a certain threshold, then a new macrophage is placed in micro-compartment (i,j) (provided that (i,j) is not already occupied by a macrophage). New macrophages are randomly assigned an age between 0 and 100 days (M_{rls}) (Furth et al., 1973). Like T cells, the age of each macrophage is incremented until it reaches its lifespan, at which time it is removed from the environment.

Macrophages move chemotactically similar to T cells, as described above in Section 3.3.3, i.e., according to random walks biased towards neighboring

[3]For simplicity we have chosen to use the same carrying capacity for all macrophages. This is another aspect of the model that could be used to introduce heterogeneity into the macrophage population in future extensions of this model.

micro-compartments with higher concentration of chemokine. However, we assume that macrophages move at slower speeds than T cells.

The rest of this section describes the rules executed for each macrophage. Additionally, the algorithmic definition of some rules are given in the appendix. Briefly, the rules represent the following processes: Resting macrophages take up bacteria and either kill them or become infected. Infected macrophages become activated only if they contain a small number (N_c) of intracellular bacteria. After the number of intracellular bacteria grows above N_c, infected macrophages are classified as chronically infected. Chronically infected macrophages are no longer able to take up and kill extracellular bacteria, nor can they be activated. Chronically infected macrophages may burst due to an excessive intracellular bacterial load, or they may be killed by T cells.

Resting macrophage rules: To reflect resting macrophage dynamics described above, the following rule is executed for each macrophage in the resting state (M_R). We assume that if there are a small number of extracellular bacteria present in the same micro-compartment as a resting macrophage (namely, less than N_{RK}—for which we use a value of 2), then the macrophage phagocytoses and kills those bacteria and remains in the resting state.

On the other hand, if there are more than N_{RK} bacteria present, then there is some small probability p_k that the macrophage still succeeds in killing N_{RK} intracellular bacteria; but it is more likely that it cannot, in which case the macrophage becomes infected (M_I) with an intracellular level of N_{RK}. The value of p_k is set to 5%, since for *M. tuberculosis* the chances that a resting macrophage can actually kill bacteria is quite low (Zahrt, 2003). This process is shown in Fig. 5, and the algorithm is shown in Appendix A.1.

Infected macrophage rules: The following rules are executed for each infected macrophage (M_I) (see the algorithm in Appendix A.2):

- Chemokine secretion: At every time-step, each infected macrophage releases a given amount $c_I = 5000$ units of chemokine into its micro-compartment. The model is invariant to changes in c_I, for $c_I > 1$.

$$C_{i,j}(t+1) = C_{i,j}(t) + c_I.$$

- Intracellular bacterial replication: Intracellular bacteria replicate within infected macrophages. The discrete intracellular growth rate α_{BI} is 0.00048/min, based on an intracellular doubling time of 24 h for *M. tuberculosis* (Paul et al., 1996). For intracellular bacterial replication α_{BI}, we use a range of values between 0.0002 and 0.0006/min:

$$B_I(t+1) = B_I(t) + \alpha_{BI} * B_I(t).$$

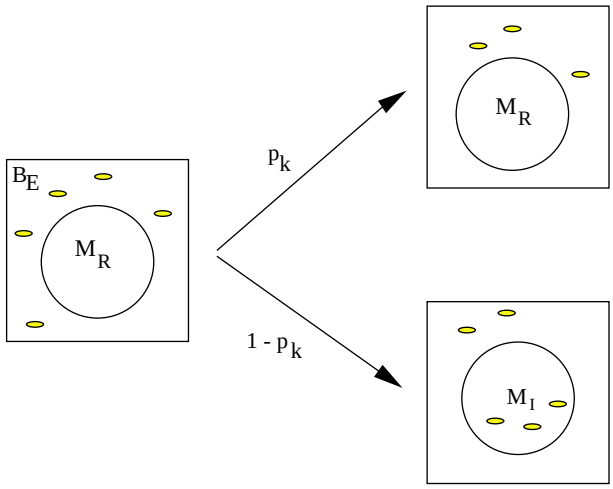

Fig. 5. Rule for resting macrophage phagocytosis. A resting macrophage can either kill bacteria and remain resting, or become infected (M_I).

- Chronic infection: The intracellular bacterial load of an infected macrophage increases over time due to the process of bacterial replication (described above). If the intracellular bacterial load exceeds a threshold N_c, the macrophage becomes chronically infected (see the arrow from M_I to M_C in Fig. 4).
- T cell activation: Macrophage activation can occur if there are T cells in or around the micro-compartment where an infected macrophage resides. Cytokines such as IFN-γ and TNF are produced by T cells and are involved in the process of macrophage activation. Instead of including cytokines in our initial formulation, we use the T cell population (that secretes these effectors) as a surrogate. This is reasonable as levels of cytokines are likely proportional to the numbers of cells that secrete them.

Macrophage activation is a function of the number of T cells in the immediate (Moore) neighborhood of an infected macrophage (with a maximum number N_{tact}), and the probability that T cells will activate a macrophage (T_{actm}). If the macrophage is activated, then it eliminates its intracellular bacterial load, and it will have a lifespan (M_{als}) of 10 days. See Fig. 6.

Chronically infected macrophage rules: The following rules are executed for each chronically infected macrophage (see the algorithm in Appendix A.3):

- Chemokine secretion: Like infected macrophages, a chronically infected macrophage secretes chemokine into its micro-compartment.
- Intracellular bacterial replication: We assume that within chronically infected macrophages, intracellular bacteria replicate logistically with respect to the

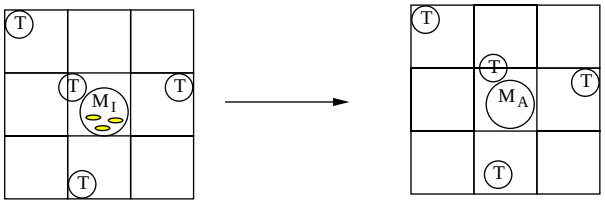

Fig. 6. Rule for activation of an infected macrophage by T cells. Note that activation occurs with a probability based on the number of T cells in the neighborhood.

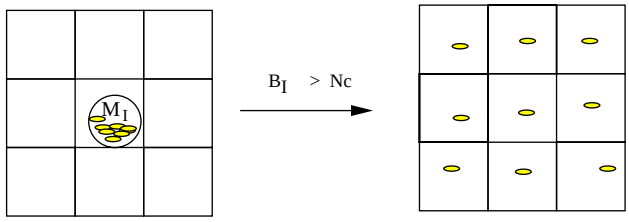

Fig. 7. Rule for bursting of a chronically infected macrophage.

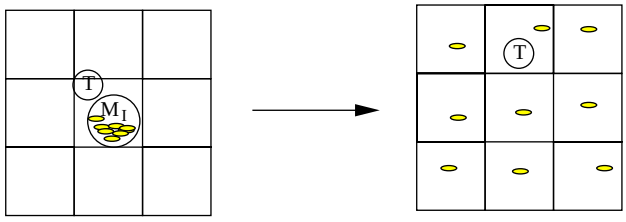

Fig. 8. Rule for T cell killing of a chronically infected macrophage.

bacterial carrying capacity of macrophages, K_{BI}.

$$B_I(t+1) = B_I(t) + \alpha_{BI} * B_I(t) * (1 - (B_I(t)/(K_{BI} + 30))).$$

We use a value of $K_{BI} = 20$ based on data from Paul et al. (1996) and Zhang et al. (1998).

- Bursting: If the intracellular bacterial load of a chronically infected macrophage exceeds the bacterial carrying capacity of macrophages (K_{BI}), the macrophage bursts and its intracellular bacteria are released. We assume that bursting spreads bacteria in the current micro-compartment as well as to neighboring micro-compartments. See Fig. 7 for an illustration.
- T cell killing: If there is a T cell in the same micro-compartment as a chronically infected macrophage, the T cell can kill the macrophage with a probability pT_k. The cytotoxic pathway via granulysin kills most of the intracellular bacteria within the cytosol of the macrophage (Lazarevic and Flynn, 2002). The other likely pathway, apoptosis, induces cell death releasing all of the intracellular bacterial pool into the environment (making them extracellular) (Bodnar et al., 2001). Since we include only generalized T cell killing processes in the model, we average the results of these two mechanisms and assume 50% of the bacteria load are killed. As with bursting, we assume that bacteria are spread to neighboring compartments by this process (see Fig. 8).

Activated macrophage rules: The following rules are executed for each activated macrophage:

- Chemokine secretion: Like infected and chronically infected macrophages, each activated macrophage secretes chemokine into its micro-compartment.
- Phagocytosis and killing of extracellular bacteria: Activated macrophages are highly efficient at phagocytosing and eliminating extracellular bacteria. We assume a certain number N_{phag} of extracellular bacteria are eliminated from a micro-compartment where an activated macrophage resides:

$$B_{Ei,j}(t+1) = B_{Ei,j}(t) - N_{phag} \geqslant 0.$$

3.3.5. Necrosis

The presence of dead or necrotic lung tissue is common in TB. Cytotoxic conditions are created when, for example, reactive nitrogen and oxygen intermediates are released from infected macrophages. These molecules are created by macrophages to kill bacterial cells in specialized compartments within macrophages; however, when macrophages die, these molecules are released into surrounding tissues and are also cytotoxic to lung tissue cells causing damage and necrosis.

We model necrosis of lung tissue by counting how many times a chronically infected macrophage bursts or is killed by a T cell in each micro-compartment (i,j). A micro-compartment (i,j) is declared to be *necrotic* if the number for bursting or T cell killings exceeds N_{necr}; we use a value of $N_{necr} = 8$. We explore the process of necrosis and its effect in other work.

3.3.6. Implementation

The ABM was implemented in C/C++. The lattice is represented by a two-dimensional array. Each element of the array contains data of macrophages, T cells, chemokine and bacteria. Objects were created for macrophages and T cells. Real variables were used for extracellular bacteria and chemokine. For each time-step we updated chemokine values. On a longer time-scale (10 min) we asynchronously update T cell movement, and on even longer time-scale (e.g. 20 min), we update macrophage movement. We also update macrophage and T cell states. This algorithm loops during a simulation time of 200 days. Each simulation took about 15 min on a Pentium Xeon 2.6 GHhz workstation. As an example, some algorithms and equations for macrophages are given in the appendix.

Table 1 summarizes all parameter values used for two distinct simulation scenarios, namely containment

Table 1
Parameter definitions for the model

Symbol	Parameter description	A	B	Units	Source
λ	Chemokine diffusion coefficient	0.64	0.65	/0.1 min	d
δ	Chemokine degradation coefficient	0.001	0.0004	/0.1 min	d
p_k	Prob. of bacteria being killed within M_R	8.51	2.36	%	e
pT_k	Prob. T cell kills a macrophage	6.31	3.61	%	e
P_{kill}	% of B_I being destroyed by killing	50	50	%	d
K_{BE}	Carrying capacity (B_E) of micro-compartment	200	200	Scalar	e
α_{BI}	Intracellular bacteria growth rate	0.00021	0.00049	/min	d
α_{BE}	Extracellular bacteria growth rate	0.00015	0.00015	/min	d
N_c	No. of intracellular bacteria defining transition to chronically infected state	10	10	Scalar	e
K_{BI}	No. of bacteria that makes a macrophage burst	20	20	Scalar	d
N_{tact}	No. of T cells needed to activate a macrophage	4	5	Scalar	e
T_{recr}	Prob. of T cell recruitment	32	12.31	%	e
T_{move}	Prob. of T cell movement, see Section 3.3.3	4.97	5.26	%	e
T_{actm}	Prob. a T cell will activate a macrophage	6	12.2	%	e
T_{ls}	T cell lifespan	3	3	days	d
T_{delay}	T cell delay	10	10	days	d
M_{recr}	Prob. of macrophage recruitment	2.11	6.82	%	e
M_{rls}	Resting macrophage lifespan	100	100	days	d
M_{als}	Activated macrophage lifespan	10	10	days	e
N_{necr}	No. of burstings to become necrotic	8	8	Scalar	e
T_{sp}	T cell speed	10	10	μm/min	d
M_{rsp}	Resting macrophage speed	1	1	μm/min	d
M_{asp}	Activated macrophage speed	0.025	0.0632	μm/min	e
M_{isp}	Infected macrophage speed	0.0007	0.0007	μm/min	e
M_{init}	Initial No. of resting macrophages	105	97	Scalar	e
N_{RK}	No. of bacteria killed by M_R	2	2	Scalar	e
N_{phag}	No. of bacteria killed by M_A	10	10	Scalar	e

Values for containment (column A) and dissemination (column B) simulations are given. Parameters *d* are from references, and *e* are estimated. See text for more information.

(Column A) and dissemination (Column B), selected from the 1000 scenarios obtained in Section 3.4.

3.4. Sensitivity and uncertainty analyses

Although we estimated biologically realistic values for a number of the parameters in the model, a number of other parameters cannot be accurately estimated from the biological literature; for instance, the probabilistic parameters used in the stochastic rules (for recruitment of T cells and macrophages, for activation of macrophages, etc.). Thus, there is a high-dimensional parameter space to explore. Uncertainty and sensitivity analysis using LHS/PRCC methods have been used in the analysis of numerous differential equation models, such as models of disease transmission (Blower and Dowlatabadi, 1994) and AIDS (Blower et al., 2002), and complex systems (Helton and Davis, 2003). However, we believe this is the first application of these methods in the context of agent-based models.

We explored the parameter space by performing an uncertainty analysis using Latin hypercube sampling (LHS) method, which is an extension of Latin square sampling. Sensitivity analysis was performed by evaluating partial rank correlation coefficients (PRCCs) (Blower and Dowlatabadi, 1994; Helton et al., 2000) for various input parameters against given outcome variables (discussed below).

We performed uncertainty and sensitivity analyses as described above for 12 parameters using LHS with 1000 samples (i.e. more than 80 samples for each parameter). Parameter ranges are given in Table 2, and a uniform distribution function was used for all parameters, as no weight for any value within the identified ranges is known. To explore the random effect of a given parameter set on output, we performed 10 simulations for both the containment and dissemination parameter sets (see Table 1 columns A and B, respectively). The results shown in Fig. 9 show little variability from stochastic parameters on the outcome within each of the two infection outcome scenarios (i.e. containment or dissemination). This result combined with the high sample size for LHS ($N = 1000$) lends confidence that each LHS simulation is among the typical output for the distinct outcomes even given the stochastic nature within those ranges.

To both qualitatively and quantitatively analyse the effects of varying parameters, we used two outcome

Table 2
Parameter ranges for LHS/PRCC analysis. All parameters have a uniform distribution

Symbol	Parameter	Min	Max	Units
λ	Chemokine diffusion coefficient	0.5	0.8	/0.1 min
δ	Chemokine degradation coefficient	0.000288	0.0011	/0.1 min
α_{BI}	Intracellular growth rate	0.0002	0.0006	/min
T_{recr}	Prob. of T cell recruitment	10	40	%
T_{move}	Prob. of T cell movement, see Section 3.3.3	1	20	%
T_{actm}	Prob. a T cell will activate a macrophage	5	20	%
M_{init}	Initial No. of macrophages	40	400	Scalar
M_{recr}	Prob. of macrophage recruitment	2	7	%
M_{asp}	Activated macrophage speed	0.0125	1	μm/ min
N_{tact}	No. of T cells needed to activate a macrophage	1	10	Scalar
p_k	Prob. of bacteria being killed by resting macrophage	1	10	%
pT_k	Prob. T cell kills a macrophage	1	10	%

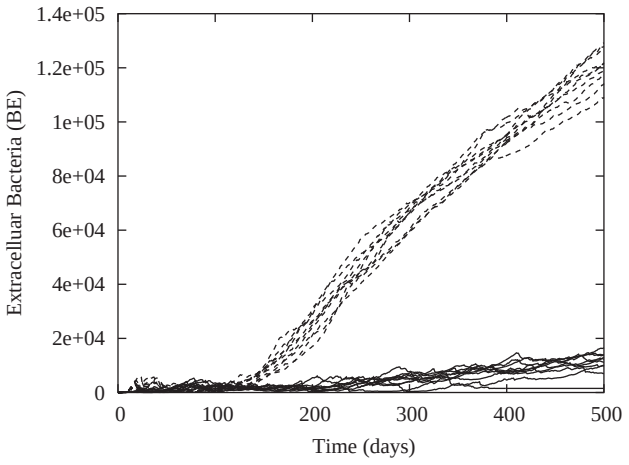

Fig. 9. Ten simulations for each outcome, containment (solid lines) and dissemination (dashed lines), are shown. The outcome variable here is extracellular bacteria load (this is also the same result for the other outcome variable, granuloma size- data not shown). These two classes of simulations are obtained from two given sets of parameters (Table 1). Simulations show little stochastic variability within each class.

variables to measure the development and spread of infection. One is total extracellular bacteria, which is used as an experimental marker of disease progression and has been used in our previous ODE models (Wigginton and Kirschner, 2001; Ganguli et al., 2004) as a predictor of infection. The second is a spatial measure that approximates the total amount of tissue to which infection has spread: the number of micro-compartments containing either an infected macrophage, a chronically infected macrophage, activated macrophages, and necrosis. We define the latter outcome variable *granuloma size* (as in Gammack et al., 2003). In future work we explore other measures for estimating granuloma size. The correlation between extracellular bacteria and granuloma size is discussed below. For brevity, we report in figures only the first measure.

4. Results

In this section, we describe results that we obtained with the model described above. We define initial conditions used for our simulations, and then outline different infection outcomes that the simulations reproduce. To better understand the dynamics leading to these outcomes, we describe in detail the early dynamics of the system and how this contributes to determining infection outcome. This leads us to examine the effects of certain key parameters. We conclude with the application of the sensitivity and uncertainty analyses that we adopted to explore the effects of variations in parameters on infection outcome.

4.1. Initial conditions

Fig. 2 depicts initial conditions used for all simulations. Some number (M_{init}) of macrophages are randomly placed on the lattice. Recall that the lattice represents 4 mm^2 of alveolar lung tissue. It has been estimated that in humans there are on the order of 10^9–10^{10} alveolar macrophages in the lung, and that there is approximately 10^8 mm^2 of alveolar surface area (Mercer et al., 1994; Stone et al., 1992). This yields estimates of 10–100 alveolar macrophages per mm^2 of tissue. Thus, we obtain a range of 40–400 for M_{init}. These macrophages are all initially in a resting state, since they represent resident alveolar macrophages before infection is introduced.

As mentioned in Section 3.3.2, a small initial infectious dose of extracellular bacteria is divided among a few micro-compartments near the center of the lattice. For the simulations described below, 16 extracellular bacteria were divided among four adjacent micro-compartments closest to the center of the lattice, i.e., $B_{E49,49}(0) = B_{E49,50}(0) = B_{E50,49}(0) = B_{E50,50}(0) = 4$. There are no T cells and no chemokine on the lattice initially.

4.2. Infection outcomes

We found that by varying parameter values within biologically reasonable ranges using the LHS method, the model reproduces stable outcomes that can be qualitatively classified into three distinct categories corresponding to distinct clinical/pathological outcomes: (1) clearance, (2) small, slow growing solid granulomas leading to containment (including granulomas containing necrotic areas either with or without bacteria), and (3) large, necrotic granulomas leading to disseminated infection.

Clearance is characterized by elimination of extracellular bacteria, absence of infected and chronically infected macrophages, and little or no necrotic tissue. Containment is characterized by the survival of extracellular bacteria in regions surrounded by a small amount of necrotic tissue, and/or slow bacterial growth within infected macrophages; however the immune response in some cases eventually eliminates infected and chronically infected macrophages. In dissemination, on the other hand, there is a large and increasing amount of necrosis, and extracellular bacteria can spread across the environment.

Fig. 9 shows typical outcomes for containment (solid lines) and dissemination (dashed lines) for the outcome variable extracellular bacteria load, each repeated 10 times with the same initial parameter values (from Table 1). Observe that the plots within each case (i.e. containment or dissemination) are clustered.

Figs. 10 and 11 show simulations representing containment and dissemination simulations, respectively, via a series of snapshots of the spatial environment. Fig. 10 shows an example of a containment simulation at days 12, 25, 50, 100, and 200 obtained with parameters from Table 1 column A; while Fig. 11 shows an example of a dissemination simulation at those same time points, with parameters from Table 1 column B. In the following section we analyse the observed dynamics in greater detail.

4.3. Early stages of infection

To better understand and isolate what drives the system towards one of the two infection outcomes discussed above, we compare the dynamics observed in Figs. 10 and 11 showing, respectively, containment and dissemination scenarios. Beginning from the initial state described above, we observe that the system typically evolves as follows.

Resident resting macrophages randomly change position, since each macrophage performs a random walk in the absence of chemokine. This is a corollary of our chemotactic movement rule. When a resting macrophage enters a micro-compartment containing extracellular bacteria, it likely becomes infected. This leads to

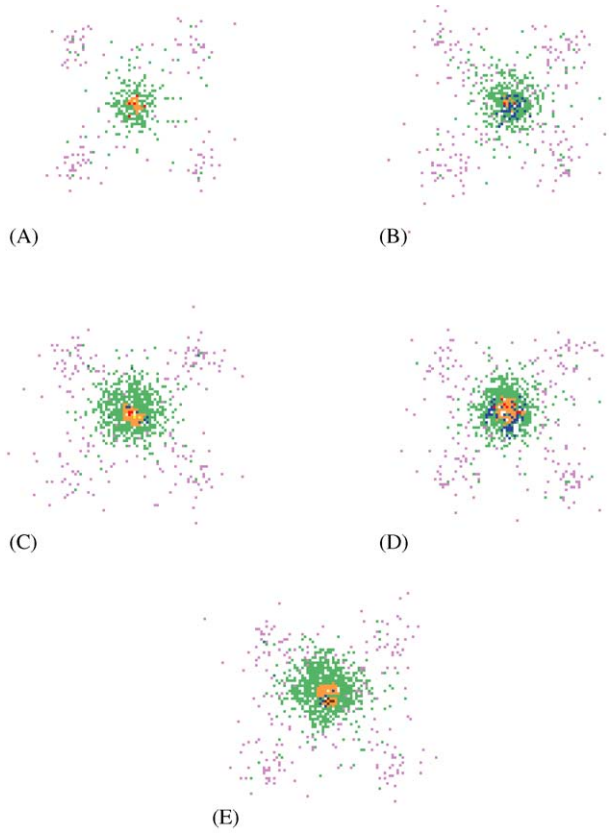

Fig. 10. (A) Granuloma showing containment at 12 days. Simulation parameters in Table 1, column A. (B) Granuloma showing containment at 25 days. (C) Granuloma showing containment at 50 days. (D) Granuloma showing containment at 100 days. (E) Granuloma showing containment at 200 days. The colors represent resting macrophages (green), activated macrophages (blue), infected macrophages (orange), chronically infected macrophages (red), T cells (pink), necrotic tissue (brown), and extracellular bacteria (yellow). Simulation movies in AVI format can be found at http://malthus.micro.med.umich.edu/lab/abm/movies/

a small number of infected macrophages, clustered near the center of the lattice. These infected macrophages release large amounts of chemokine (not shown). Chemokine diffusion creates a chemokine gradient on the lattice. This chemokine gradient directs movement of the remaining resident resting macrophages already on the lattice, since their random walks are biased towards higher chemokine levels. Also, recruitment of additional resting macrophages is initiated when sufficient levels of chemokine diffuse to the source micro-compartments. These resting macrophages also migrate toward the source of chemokine.

Meanwhile, intracellular bacteria replicate within infected macrophages, which become chronically infected. These dynamics result is an initial "granuloma structure" consisting of a small number of chronically infected macrophages surrounded by resting macrophages. This can be seen in both snapshots at day 12 in Figs. 10A and 11A. In non-human primate models,

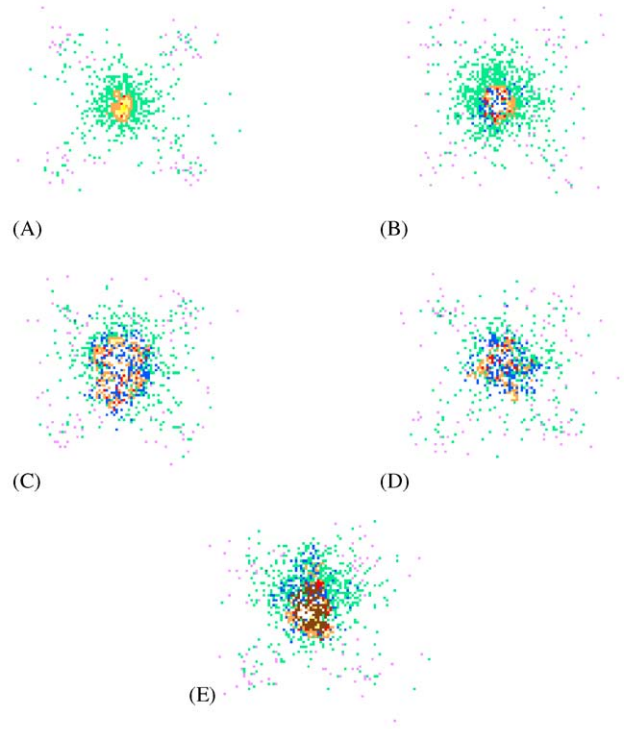

Fig. 11. (A) Granuloma showing dissemination 12 days. Simulation parameters in Table 1, column B. (B) Granuloma showing dissemination at 25 days. (C) Granuloma showing dissemination at 50 days. (D) Granuloma showing dissemination at 100 days. (E) Granuloma showing dissemination at 200 days. The colors represent resting macrophages (green), activated macrophages (blue), infected macrophages (orange), chronically infected macrophages (red), T cells (pink), necrotic tissue (brown), and extracellular bacteria (yellow). Simulation movies in AVI format can be found at http://malthus.micro.med.umich.edu/lab/abm/movies/

granuloma structures are observed as early as two weeks after infection (J. Flynn, personal communication).

As intracellular bacteria continue to replicate within chronically infected macrophages, macrophages eventually burst when their carrying capacity is reached. This spreads extracellular bacteria to neighboring micro-compartments where extracellular bacteria is phagocytosed by neighboring resting macrophages. This results in a new round of infected macrophages.

In both settings, after a delay of 10 days, T cells enter the lattice due to chemokine-driven recruitment. We enforce such a delay to account for the time it takes for antigen-presenting cells (such as dendritic cells) to migrate to the lymph node and prime T cells, and for T cells to then migrate from the lymph node to the site of infection.[4] The length of this delay is important since it affects the spatio–temporal distribution of T cells with respect to the growing granuloma structure of infected and resting macrophages, and below we study the effects of variations to the delay length. The spatio–temporal distribution of T cells is significant, and we also discuss this below.

Chemotactic movement of T cells means that, like macrophages, they tend to be recruited and move toward the edges of granuloma. Moreover, according to movement rule of T cells, there is a possibility for T cells to move into micro-compartments where macrophages reside.

Hence, some T cells penetrate the cluster of resting macrophages surrounding chronically infected macrophages. This can be seen in both Figs. 10B and 11B.

The interplay between T cell migration and bursting of chronically infected macrophages leads to a key dynamic influencing spread or containment of infection: What happens when one chronically infected macrophage bursts and causes a new round of infections in neighboring resting macrophages? There are two possibilities. If T cells have migrated to the immediate neighborhood of a chronically infected macrophage when bursting occurs, these T cells may *activate* the newly infected macrophage(s), contributing to control of infection. On the other hand, if there are no T cell agents nearby, infected macrophages may progress to a chronic infection state, contributing to infection spread.

4.4. Later states of infection

Fig. 10B (Containment scenario at 25 days) shows activated macrophages (in blue) densely concentrated in the center of the granuloma. Fig. 11B (Dissemination scenario at 25 days) also shows activated macrophages but many more infected and chronically infected macrophages.

Fig. 10C (Containment scenario at 50 days) shows infected macrophages surrounded by resting macrophages, a few extracellular bacteria in the center of the granuloma, and a ring of T cells surrounding macrophages as observed in typical granulomas. On the other hand, Fig. 11C (Dissemination scenario at 50 days) shows a larger granuloma with more infected and activated macrophages at the edges of the granuloma; clearly bacteria are not being contained and the granuloma continues to grow.

Fig. 10D (Containment scenario at 100 days) shows infected macrophages at the center of the granuloma, with activated macrophages in a ring, containing the spread of the infection. Conversely, Fig. 11D (Dissemination scenario at 100 days) shows many activated macrophages in a diffuse granuloma structure; bacteria are not being contained.

Fig. 10E (Containment scenario at 200 days) shows infected macrophages walled off by macrophages. On

[4]Future extensions of this model could include these antigen-presenting cells and T cell activation in the lymph node, thus developing an agent-based version of the two-compartmental model of Marino and Kirschner (2004).

the other hand, Fig. 11E (Dissemination scenario at 200 days) shows many infected macrophages at the periphery, inducing spread of bacteria outside the granuloma. Necrotic tissue appears due to the high frequency of macrophages bursting and killing in the area, an indication of a strong inflammatory response. Many activated macrophages are found over the site.

A specific set of parameters, identified through uncertainty and sensitivity analyses, controls the distinct outcomes observed. We analyse each of these parameters in the next section.

4.5. Results of uncertainty and sensitivity analysis

To explore the role of parameter values on the dynamics observed, we perform detailed uncertainty and sensitivity analyses as outlined above. To this end, we identified a group of parameters we consider important to control bacterial load. Granuloma size, obtained as the sum of infected, chronically infected, activated macrophages and necrosis, is highly correlated with extracellular bacteria (correlation value of 0.966, $p<0.001$ at 500 days). Table 3 shows a list of these parameters and also gives temporally dependent PRCC values for each parameters related to the outcome variable, B_E. Below we discuss the influence of each parameter on infection outcome in more detail.

Because TB is a long-term disease (even if containment leads to latency), we explore our sensitivity analysis beyond the typical time-frame it takes for a granuloma to form (14–100 days) to up to 500 days. This yields insight into which mechanisms are important to long-term granuloma maintenance rather than granuloma formation. Table 3 presents PRCC values for key parameters out to the 500 day time point for comparison. Some parameters gain (or lose) significance at that later time point and this lends insight into which processes are involved in maintenance of long-term latent infection.

4.5.1. Chemokine diffusion coefficient, λ, and Chemokine decay coefficient, δ

The chemokine diffusion coefficient λ is positively correlated with extracellular bacteria (B_E), meaning higher chemokine diffusion rates enhance total extracellular bacterial load (or granuloma size) (see Table 3). On the other hand, the chemokine decay rate δ is negatively correlated with B_E. An interesting result is that δ has its highest negative correlation around 30 days after infection. This result suggests that granuloma growth could be reduced if the half-life of key chemokines are reduced, or their function is blocked, with the strongest effect expected at 30 days after infection. This effect aligns with the observed crowding effects of macrophages as discussed further below.

4.5.2. Intracellular bacterial growth rate, α_{BI}

One interesting feature of *Mycobacterium* is their slow growth rate. Their doubling time is order of magnitudes slower than most other pathogenic bacteria. This interesting feature surfaces as a determinant of infection outcome. In fact, the intracellular bacteria growth rate is strongly correlated with extracellular bacterial load and shifts from positive to negative over time. During the first days of infection, large α_{BI} allows the granuloma to grow fast, in particular, between days 5 and 15 post-infection, with a correlation peak of $+0.98$ at day 12 (Table 3). However, we observe a sign shift in the PRCC value around the 25th day of infection, becoming significant negatively correlated at around the 30th day of infection. At day 60, the PRCC value between α_{BE} and bacteria (B_E) is -0.48. Then, there is another sign shift around day 150 post-infection, with PRCC value 0.45 at 180 days and 0.31 at 500 days (see Table 3).

Table 3
PRCC values of parameters that are significantly positively or negatively correlated with total extracellular bacteria (B_E), according to LHS/PRCC analyses

Symbol	Parameter description	Days				
		12	30	60	180	500
λ	Chemokine diffusion coefficient	ns	0.18	0.13	ns	0.13
δ	Chemokine decay coefficient	ns	−0.29	−0.15	ns	−0.19
α_{BI}	Intracellular growth rate	0.98	−0.14	−0.48	0.45	0.31
T_{recr}	Prob. of T cell recruitment	ns	−0.36	−0.27	−0.16	−0.31
T_{move}	Prob. of T cell movement, see Section 3.3.3	ns	−0.65	−0.54	−0.61	−0.57
T_{actm}	Prob. of T cell activates a macrophage	ns	−0.24	−0.16	ns	−0.15
M_{init}	Initial No. of macrophages	ns	0.40	0.21	ns	ns
M_{recr}	Prob. of macrophage recruitment	ns	0.56	0.61	0.67	0.75
M_{asp}	Activated macrophage speed	ns	0.31	0.32	ns	ns

Note that correlations change over time. All values indicated have significance $p<0.001$, n.s. is non-significant. Parameter sets used were from Tables 1 and 2.

These results indicate that between the first and second month post infection, *M. tuberculosis* generates larger granulomas when it grows more slowly (within the biological ranges explored in Table 2).

4.5.3. Rate of macrophage recruitment, M_{recr} and initial number of macrophages M_{init}

The rate of macrophage recruitment, M_{recr}, is represented in the model as a probability. At each time-step and at each source compartment, a new macrophage is introduced onto the lattice with probability M_{recr}. We observe strong positive correlations between M_{recr} and the two outcome variables, total extracellular bacteria and granuloma size (see Fig. 12). Increased recruitment of macrophages tends to be detrimental to infection outcome in this model. Increasing this parameter leads to a greater number of resting macrophages crowding around the granuloma center, being susceptible to infection; as a result the "lymphocyte cuff" of T cells is pushed further out, allowing infection to incubate and spread within granuloma structure. This can be interpreted as resting macrophages crowding out T cells. In other words, macrophages create a barrier that prevents T cells from migrating towards the center of the granuloma and activating macrophages. Recall that activated macrophages have the ability to kill large amounts of extracellular bacteria. For similar reasons the initial number of macrophages M_{init} is also positively correlated with extracellular bacteria B_E (see Table 3) and granuloma size (data not shown) as too many initial macrophages can induce the same phenomenon.

From our observations it is expected that a balance in the number of macrophages present in the granuloma exists: an optimal number of macrophages large enough to wall off spread of bacteria, but not too large that it blocks access of T cells towards the center of the granuloma.

4.5.4. Rate of T-cell recruitment (T_{recr}) and probability of T-cell movement (T_{move})

Macrophage activation is important to controlling granuloma size. In the model, macrophage activation is dependent on T cell abundance near infected macrophages. Thus, we expected both the rate of T cell recruitment (T_{recr}) and the probability of T-cell movement (T_{move}) to be important parameters. In particular, we expected them to demonstrate strong negative correlations with the outcome variables. However, our results show that T_{move} is more strongly correlated with both granuloma size or total extracellular bacteria than is T_{recr}.

Our results indicate (as shown in Table 3) that the number of T cells (as determined by the value of the parameter T_{recr}) is not as significant for halting the spread of infection. Rather, what is more important is how well T cells are able to navigate towards the center of the granuloma. T cell movement (T_{move}) is negatively correlated with extracellular bacteria (B_E) (see Fig. 13). If T cells have an increased ability to move toward the center of the granuloma (reflected in our model by the parameter T_{move}), then they have increased opportunities to activate macrophages and hence limit infection spread.

These findings likely have important implications. There must exist a balance between the number of macrophages and T cells present in the granuloma. Macrophages crowd around the initial site of infection, and in the absence of T cells, become infected. This triggers a positive feedback loop of infection and bursting, leading to infection spread, as measured by either outcome variable (large granuloma size or numbers of extracellular bacteria). This occurs when there are so many resting macrophages clustered around the local site of infection that they prevent T cells from moving close enough to the infection site to activate macrophages.

4.5.5. Other significant parameters

Our uncertainty and sensitivity analyses revealed that several other parameters are significantly correlated with the total extracellular bacteria (B_E) (Table 3), indicating that they have a strong influence on spread of infection. For example, the rate of activated macrophage movement is negatively correlated with total extracellular bacteria. This likely follows since increasing the rate at

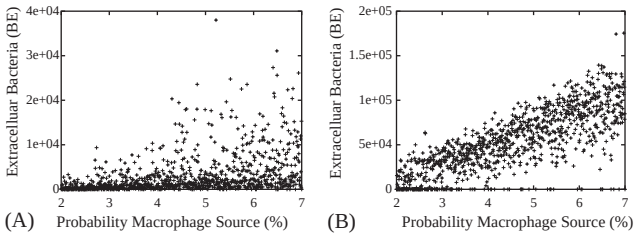

Fig. 12. The relationship between probability of recruiting macrophages (M_{recr}) and extracellular bacteria (B_E), at 62 and 500 days, from 1000 simulations. Both have significance with $p<0.001$. (A) at 62 days with PRCC = 0.61, and (B) at 500 days with PRCC = 0.75.

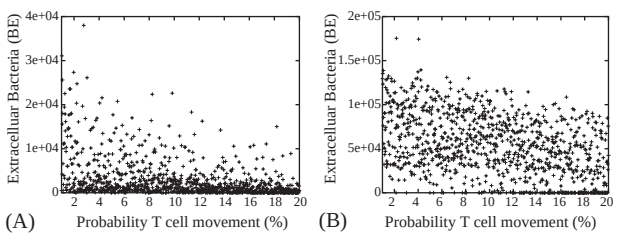

Fig. 13. The relationship between probability of T cell movement (T_{move}) and total extracellular bacteria (B_E), at 62 and 500 days, from 1000 simulations. (A) at 62 days, PRCC = −0.56, and (B) at 500 days, PRCC = −0.57. Both have significance with $p<0.001$.

which activated macrophages change location implies they reach more micro-compartments containing extracellular bacteria. However, since they are not able to clear all bacteria in one micro-compartment before they move to another location, they leave behind extracellular bacteria that could then infect new resting macrophages. On the other hand, the initial number of resting macrophages is positively correlated with total extracellular bacteria. Increasing the initial number of resting macrophages has a similar effect as increasing M_{recr}, as described above.

4.6. Adaptive immunity delay, T_{delay}

In the absence of prior infection or vaccination, the adaptive immune response takes anywhere from 5–10 days to develop activated immune cells specific for responding to the pathogen in question (Lurie, 1964; Janeway, 2001; Jenkins et al., 2001; Medzhitov and Janeway, 2000). In our simulations, we do not capture this delay through a mechanistic priming and trafficking between lymph nodes and the site of infection (we explore this in other work—Marino and Kirschner, 2004). Instead, we capture this effect by imposing a constant time delay before T cells begin arriving at the infection site. To study the impact of variations in this delay we vary the time for initial arrival of effector T cells to the site between 0 and 25 days (T_{delay}) (see Fig. 14).

There are two scenarios to consider. First, we consider the parameter set that leads to containment and vary the T cell arrival time (Fig. 14, Panel A). Fig. 14 shows that the outcome variable (B_E) is significatively affected when T cells arrive in the first few days of infection (i.e. no delay). In this situation we observe complete clearance of bacteria. As most individuals experience latent infection (95%) then we can likely assume their granulomas are containing or clearing infection. This implies that an important role could be played by successful vaccination of most individuals, ensuring an early T cell response upon infection. However, when using the parameter set that leads to dissemination, lower numbers of bacteria are noted rather than clearance (Fig. 12, Panel B). This suggest that for a given parameter set, T cell immunity is crucial at the beginning of the infection. T cells arriving at later times (5, 10, or 20 days) do not have the same effect as when they arrive earlier (<5 days). At the later time, other mechanisms are more important in controlling infection such as macrophage density and T cell parameters (discussed above), and they must work in concert to control infection, with T cells playing a key part in this dynamic. When other parts of the system are prone to containment, T cells can exhibit their greatest effect early in infection (Fig. 14).

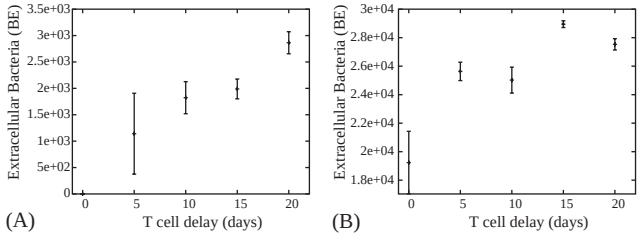

Fig. 14. The effect of varying T cell arrival delay (T_{delay}) on extracellular bacteria (B_E), using parameters set leading to containment (A) and dissemination (B) from Table 1. Data observed at 200 days of simulation $N = 10$.

5. Discussion

In this paper, we have presented an agent-based model of the adaptive immune response to *M. tuberculosis* infection. In particular, we focused on the unique spatial structure that develops during this response, and simulate the formation of a granuloma. We applied uncertainty and sensitivity analyses (LHS/PRCC) with respect to the parameter space for the first time in this setting. The parameters discussed are grouped into those that govern chemokine and cytokine dynamics, those that govern host cell dynamics, namely T cells and macrophages, and those that govern bacterial growth rates.

5.1. Chemokines and cytokines

Chemokines are important molecules governing granuloma formation (Flynn and Chan, 2001). Chemokines are small proteins (8–10 kDa) and are a subset of a general group of effector molecules known as cytokines. These chemoattractants serve to draw macrophages and T cells to the infection site. Human macrophages infected with *M. tuberculosis* produce several chemokines such as: CCL, CCL3, CCL4, and CCL5, among others (Scott et al., 2003). These molecules create a concentration gradient for macrophages and T cells. However, recruiting appropriate immune cells to the site of infection is necessary but insufficient to control infection outcome.

Our results show that an increase in chemokine diffusion increases granuloma size. An opposite effect is observed for chemokine degradation, where rapid degradation decreases granuloma size. This result implies that a balance must exist between chemokines attracting macrophages and T cells to kill bacteria, while attempting to maintain smaller granuloma size (i.e. less tissue damage). Conversely, an increase in the concentration and lifespan of chemokines increases granuloma size. Taken together these results imply that if it were possible to control chemokines in this way it could prevent macrophage overcrowding. We have included a

very generalized chemokine in this model and our goal is to consider the effects of more specific chemokines in future work.

Cytokines serve as modulators of immune cell behavior. These include IFN-γ, TNF, IL-2, IL-12, among others (Flynn and Chan, 2001). There is an established complex regulation by TNF such that in the absence of this cytokine a chemokine gradient is not formed, cell migration fails, and granulomas do not form properly (Mohan et al., 2001). In this model we have used the T cells that produce cytokines as surrogates for the effector molecules they secrete. The relevance of TNF and other specific effectors are the subject of our future work.

5.2. *Mycobacterium tuberculosis*

M. tuberculosis is one of the oldest pathogens known to humans. It has evolved to be the most successful pathogen in that one third of the world is infected. It has a stable genome (Victor et al., 1997) and a curiously slow growth. Because of the stability of this organism, we place the major emphasis on the host in determining infection outcomes. However, one of the most interesting results obtained with our analyses was the shift in the sign (positive to negative) of the correlation coefficient over time regarding the influence of the intracellular bacterial growth rate on granuloma size (or bacterial load). Early in infection, high growth rates are favorable for granuloma growth, but between the 1st and 3rd month of infection (Section 4.5.2), granuloma grow larger when *Mycobacterium* growth rates are slowest. This counterintuitive result is obtained from the complex dynamics between T cells, macrophages and bacteria that occur. This confirms the importance of the slow mycobacterial growth rate as part of its virulence, and this is the first time this result has been observed through analyses of this type.

5.3. *Macrophages*

Macrophages play dual roles in Mtb infection. In their resting state, they take up extracellular bacteria and provide an ideal growth environment, yet in their activated state are able to take up and destroy bacteria. Thus, there exists a balance regarding macrophage numbers. Too many resting macrophages provide unlimited shelter to bacteria and crowd the granuloma preventing cell–cell interactions that could lead to activation and bacterial containment. Too many activated macrophages can lead to severe tissue damage through release of cytotoxic factors (such as reactive oxygen and nitrogen intermediates).

Even the speed of infected macrophages can be important in controlling granuloma growth. Slow movement of infected macrophage allows them to remain in a location longer allowing them to either become activated and kill their internalized bacteria, or to be killed by cytotoxic T lymphocytes (CTL) action. If they move too fast, they may evade these actions leading to disseminated infection.

5.4. *T cells*

From uncertainty and sensitivity analyses we observe that the parameter governing T cell movement is more significant to granuloma growth (or extracellular bacterial numbers) than the number of T cells recruited. This indicates that the spatial distribution of T cells in a developing granuloma is more important than merely their raw numbers. Studies in mice without TNF show that, while cell numbers are the same as normal mice, their spatial distribution within the granuloma is diffuse, forming disorganized granulomas (Flynn and Chan, 2001), supporting our findings. Curiously, our results indicate that the timing of T cell recruitment does not independently determine infection outcome, but works in concert with other parameters in the system. If the system is biased toward a containment scenario, then the rate and timing of T cell recruitment can influence the timing of bacterial control. Thus, these results could be applied to vaccine or treatment settings. However, if the system is biased toward a weaker response, then the system will behave almost independent of early T cell dynamics.

The rules of macrophage activation by T cells are a first approximation to a more complex phenomena. In actuality the direct role of T cells in activating macrophages is facilitated by both IFN-γ secretion as well as cell–cell interactions. It may be the case that once IFN-γ is included into the model in a more direct and mechanistic fashion, the importance of macrophage activation mediated by IFN-γ balanced with T cell interactions will be observed. This is the focus of our future work.

5.5. *Final comments*

In summary, the development of a simple model to explore granuloma formation to determine function has yielded key results that require further testing through both theoretical and experimental approaches. A more detailed model including specific cytokines and chemokines and their mechanisms will likely uncover deeper layers of this complex system. Our results here imply that indeed an agent-based approach is an appropriate tool for exploring this complex spatio–temporal system. However, it is important to determine differences between different mathematical approaches exploring the same system to determine to what extent information is revealed at different scales. In other work we draw this comparison (Gammack et al., 2004).

Acknowledgements

This work was supported by NIH grant No. R01HL68526. The authors thank Dr. Joanne Flynn, Dr. John Chan, Dr. Steven Kunkel, Dr. Stephan Ehlars, Dr. Steven Chensue, Dr. Tom Kepler, Dr. David Gammack and Dr. Simeone Marino for helpful discussions.

Appendix A

This appendix includes a sample of the algorithms we implemented for the rules described for resting, infected and chronically infected macrophages in Section 3. These algorithms were coded in C/C++ and implemented on a LINUX workstation.

A.1. Resting macrophages rules

RESTING MACROPHAGES RULES ()
if $B_Ei,j(t) \leqslant N_{RK}$ **then**
$B_Ei,j(t+1) = (B_Ei,j(t) - N_{RK}) \geqslant 0$
return M_R, Resting macrophage
endif
if $B_Ei,j(t) > N_{RK}$ **then**
$r \leftarrow$ *RandomUniform*[0, 100]
if $r \leqslant p_k$ **then**
$B_Ei,j(t+1) = (B_Ei,j(t) - N_{RK})$
M_R succeeds in killing the bacteria and remains in resting state
return M_R, Resting macrophage
else
$B_Ei,j(t+1) = (B_Ei,j(t) - N_{RK})$
$B_Ii,j(t+1) = N_{RK}$
M_R does not succeed in killing bacteria
The macrophage is infected.
return M_I, Infected macrophage
endif
endif

A.2. Infected macrophages rules

INFECTED MACROPHAGES RULES ()
Chemokines release by macrophages:
$C_{i,j}(t+1) = C_{i,j}(t) + c_I$
Intracellular bacterial replication:
$B_I(t+1) = B_I(t) + \alpha_{B_I} * B_I(t)$
Chronic infection:
if $B_I(t) \leqslant N_c$ **then**
return M_C, Chronically infected macrophage
endif
Macrophage activation:
if $B_I(t) \leqslant N_c$ **then**
$N_T =$ Number of T cells in the neighborhood
if $N_T > N_{tact}$ **then**
$N_T = N_{tact}$
endif
If the macrophage is activated, then it eliminates its intracellular bacterial load:
$r \leftarrow$ *RandomUniform*[0, 100]
if $r < (N_T * T_{actm}) \leqslant 100$ **then**
$B_Ii,j = 0$
return M_A, Activated Macrophage
else
return M_I, Infected Macrophage
endif
endif

A.3. Chronically infected macrophages rules

CHRONICALLY INFECTED MACROPHAGES RULES ()
Chemokines release:
$C_{i,j}(t+1) = C_{i,j}(t) + c_I$
Intracellular bacterial growth:
$B_I(t+1) = B_I(t) + \alpha_{B_I} * B_I(t)/(1 + (B_I(t)/(K_{B_I} + 30)))$
Bursting:
if $B_I(t) > K_{BI}$ **then**
$B_{Ei-1,j}(t+1) = B_{Ei-1,j}(t) + B_I(t)/9$
$B_{Ei+1,j}(t+1) = B_{Ei+1,j}(t) + B_I(t)/9$
$B_{Ei-1,j+1}(t+1) = B_{Ei-1,j+1}(t) + B_I(t)/9$
$-etc.$
Macrophage is eliminated
return *Death*
endif
T cell killing:
if $(B_I(t) \leqslant K_{BI})$ *and* $\exists$ *T-cell at* (i,j) **then**
$r \leftarrow$ *RandomUniform*[0,100]
if $r < (pT_k)$ **then**
$B_Ii,j(t) = (P_{kill}/100) * B_Ii,j$
$B_{Ei-1,j}(t+1) = B_{Ei-1,j}(t) + B_I(t)/9$
$B_{Ei+1,j}(t+1) = B_{Ei+1,j}(t) + B_I(t)/9$
$B_{Ei-1,j+1}(t+1) = B_{Ei-1,j+1}(t) + B_I(t)/9$
$-etc.$
Macrophage is eliminated
return *Death*
else
return M_C, Chronic Macrophage
endif
endif

References

Alarcon, T., Byrne, H., Maini, P., 2001. A cellular automaton model for tumour growth in inhomogeneous environment. J. Theor. Biol. 225, 257–274.

An, G., 2001. Agent-based computer simulation and SIRS: building a bridge between basic science and clinical trials. Shock 16, 266–273.

Anderson, A., Chaplain, M., 1998. Continuous and discrete mathematical models of tumour-induced angigenesis. Bull. Math. Biol. 60, 857–899.

Axelrod, R., 1997. The Complexity of Cooperation: Agent-Based Models of Competition and Cooperation. Princeton University Press, Princeton, NJ.

Blower, S., Gershengorn, Grant, R., 2002. A tale of two futures: HIV and antiretroviral therapy in San Francisco. Science 287, 650–654.

Blower, S.M., Dowlatabadi, H., 1994. Sensitivity and uncertainty analysis of complex models of disease transmission: an HIV model, as example. Int. Stat. Rev. 62 (2), 229–243.

Bodnar, K., Serbina, N., L., F.J., 2001. Fate of *Mycobacterium tuberculosis* within murine dentritic cells. Infect. Immunol. 69, 800–809.

Capuano, S., Croix, D., Pawar, S., Zinovik, A., Myers, A., Lin, P., Bissel, S., Fuhrman, C., Klein, E., Flynn, J., 2003. Experimental *Mycobacterium tuberculosis* infection of cynomolgus macaques closely resembles the various manifestations of human *M. tuberculosis* infection. Infect. Immun. 71, 5831–5844.

Celada, F., Seiden, P.E., 1992. A computer model of cellular interactions in the immune system. Immunol. Today 13, 56–61.

Comstock, G., 1982. Epidemiology of tuberculosis. Am. Rev. Respir. Dis. 125, 8–15.

Dannenberg, A., Rook, G., 1994. Pathogenesis of pulmonary tuberculosis: an interplay of tissue-damaging and macrophage-activating immune responses—dual mechanisms that control bacillary multiplication. In: Bloom, B. (Ed.), Tuberculosis: Pathogenesis, Protection, and Control. ASM Press, Washington, DC.

Edelstein-Keshet, L., Spiros, A., 2002. Exploring the formation of Alzheimer's disease senile plaques in silico. J. Theor. Biol. 216, 301–326.

Epstein, J., Axtell, R., 1996. Growing Artificial Societies: Social Science From the Bottom Up. Brookings Institution Press, Washington, DC.

Ermentrout, G., Edelstein-Keshet, L., 1993. Cellular automata approaches to biological modeling. J. Theor. Biol. 160, 97–133.

Flynn, J., Chan, J., 2001. Immunology of tuberculosis. Annu. Rev. Immunol. 19, 93–129.

Flynn, J., Ernst, J., 2000. Immune responses in tuberculosis. Curr. Opin. Immunol. 12, 432–436.

Francis, K., Palsson, B., 1997. Effective intracellular communication distances are determined by the relative time constants for cyto/chemokine secretion and diffusion. Proc. Nat. Acad. Sci. 94, 12258–12262.

Furth, R.V., Dulk, M.D.-D., Mattie, H., 1973. Quantitative study on the production and kinetics of mononuclear phagocytes during an acute inflammatory reaction. J. Exp. Med. 138, 1315.

Gammack, D., Doering, C., Kirschner, D., 2003. Macrophage response to *Mycobacterium tuberculosis* infection. J. Math. Biol. 48, 218–242.

Gammack, D., Ganguli, S., Marino, S., Segovia-Juarez, J., Kirschner, D., 2004. Understanding granuloma formation using different mathematical models and biological scales. SIAM Multiscale Modeling Simulation, to appear.

Ganguli, S., Gammack, D., Kirschner, D., 2004. A metapopulation model of granuloma framework in the lung during infection with *Mycobacterium tuberculosis*, submitted.

Grimm, V., 1999. Ten years of individual-based modelling in ecology: what have we learned, and what could we learn in the future? Ecological Modelling 115, 129–148.

Grosset, J., Truffot-Pernot, C., Cambau, E., 2000. Bacteriology of tuberculosis. In: Reichman, L.B., Hershfield, E.S. (Eds.), Tuberculosis: A Comprehensive International Approach. Dekker, New York.

Helton, J., Davis, F., 2003. Latin hypercube sampling and the propagation of uncertainty in analyses of complex systems. Reliab. Eng. Syst. Safety 81, 23–69.

Helton, J., Davis, Fredie, J., 2000. Sampling-based methods. In: Saltelli, A., Chan, K., Scott, E.M. (Eds.), Sensitivity Analysis. Wiley, New York, pp. 101–154.

Janeway, C., 2001. Immunobiology 5: The Immune System in Health and Disease. Garland Pub., New York.

Jenkins, M., Khoruts, A., Ingulli, E., Mueller, D., McSorley, S., Reinhardt, R., Itano, A., Pape, K., 2001. *In vivo* activation of antigen-specific CD4 T cells. Annu. Rev. Immunol. 19, 23–45.

Kansal, A., Torquato, S., Harsh, G., Chiocca, E., Deisboeck, T., 2000a. Cellular automaton of idealized brain tumor growth dynamics. BioSystems 55, 119–127.

Kansal, A., Torquato, S., Harsh, G., Chiocca, E., Deisboeck, T., 2000b. Simulated brain tumor growth dynamics using a three-dimensional cellular automaton. J. Theor. Biol. 203, 367–382.

Kreft, J., Booth, G., Wimpenney, J., 1998. Bacsim, a simulator for individual-based modelling of bacterial colony growth. Microbiology 144, 3275–3287.

Kreft, J., Picioreanu, C., Wimpenny, J., van Loosdrecht, M., 2001. Individual-based modelling of biofilms. Microbiology 147, 2897–2912.

Krombach, F., Munzing, S., Allmeling, A., Gerlach, J., Behr, J., Dorger, M., 1997. Cell size of alveolar macrophages: an interspecies comparison. Environ. Health Perspect. 105 (5), 1261–1264.

Lazarevic, V., Flynn, J., 2002. CD8+ T cells in tuberculosis. Am. J. Respir. Crit. Care. Med. 166, 1116–1121.

Lukacs, N., Chensue, S., 1996. The role of chemokines in granulomatous disease. In: Koch, A.E., Strieter, R.M. (Eds.), Chemokines in Disease. R.G. Landes, Austin.

Lurie, M., 1964. Resistance to tuberculosis: experimental studies in native and acquired defensive mechanisms. Harvard University Press, Cambridge, MA.

Mansury, Y., Deisboeck, T., 2003. The impact of "search precision" in an agent-based tumor model. J. Theor. Biol. 224, 325–337.

Mansury, Y., Kimura, M., Lobo, J., Deisboeck, T.S., 2002. Emerging patterns in tumor systems: simulating dynamics of multicellular clusters with an agent-based spatial agglomeration model. J. Theor. Biol. 219, 343–370.

Marino, S., Kirschner, D., 2004. The human immune response to *Mycobacterium tuberculosis* in lung and lymph node. J. Theor. Biol. 227, 463–486.

Marino, S., Pawar, S., Fuller, C.L., Reinhart, T.A., Flynn, J.L., Kirschner, D.E., 2004. Dendritic cell trafficking and antigen presentation in the human immune response to *Mycobacterium tuberculosis*. J. Immunol. 173, 494–506.

Markus, M., Bohm, D., Schmick, M., 1999. Simulation of vessel morphogenesis using cellular automaton. Math. Biosci. 156, 191–206.

McDonough, K., Kress, Y., Bloom, B., 1993. Pathogenesis of tuberculosis: interaction of *Mycobacterium tuberculosis* with macrophages. Infect. Immun. 61, 2763–2773.

Medzhitov, R., Janeway, C., J., 2000. Innate immunity. N. Engl. J. Med. 343 (5), 338–344.

Mercer, R., Russell, M., Roggli, V., Crapo, J., 1994. Cell number and distribution in human and rat airways. Am. J. Res. Cell Mol. Biol. 10, 613–624.

Miller, M., Wei, S., Calahan, M., Parker, I., 2003. Autonomous T cell trafficking examined in vivo with intravital two-photon microscopy. Proc. Nat. Acad. Sci. 100, 26045–26049.

Mohan, V., Scanga, C., Yu, K., Scott, H.M., Tanaka, K.E., Tsang, E., Flynn, J.L., Chan, J., 2001. Effects of tumor necrosis factor alpha on host immune response in chronic persistent tuberculosis: possible role for limiting pathology. Infect. Immun. 69, 1847–1855.

North, R., Izzo, A., 1993. Mycobacterial virulence: virulent strains of *Mycobacterium tuberculosis* have faster in vivo doubling times and are better equipped to resist growth-inhibiting functions of macrophages in the presence and absence of specific immunity. J. Exp. Med. 177, 1723.

Orme, I., Cooper, A., 1999. Cytokine/chemokine cascades in immunity to tuberculosis. Immunol. Today 20 (7), 307–312.

Paul, S., Laochumroonvoranpong, P., Kaplan, G., 1996. Comparable growth rates of virulent and avirulent *Mycobacterium tuberculosis* in human macrophages in vitro. J. Infect. Dis. 177, 1723.

Perelson, A.S., 2002. Modelling viral and immune system dynamics. Nature Rev. Immunol. 2 (1), 28–36.

Qi, A., Zheng, X., Du, C., An, B., 1993. A cellular automaton model of cancerous growth. J. Theor. Biol. 161, 1–12.

Sadek, M., Sada, E., Toossi, Z., Schwander, S., Rich, E., 1998. Chemokines induced by infection of mononuclear phagocytes with mycobacteria and present in lung alveoli during active pulmonary tuberculosis. Am. J. Respir. Cell Mol. Biol. 19, 513–521.

Saunders, B., Cooper, A., 2000. Restraining mycobacteria: role of granulomas in mycobacterial infections. Immunol. Cell Biol. 78, 334–341.

Schelling, T., 1969. Models of segregation. Am. Econ. Rev. Pap. Proc. 59, 488–493.

Schelling, T., 1978. Micromotives and Macrobehavior. Norton

Scott, H.M., Chan, J., Flynn, J., 2003. Chemokines and tuberculosis. Cytokine Growth Factor Rev. 14, 467–477.

Seiden, P.E., Celada, F., 1992. A model for simulating cognate recognition and response in the immune system. J. Theor. Biol. 158, 329–340.

Seiler, P., Aichele, P., Bandermann, S., Hauser, A., Lu, B., Gerard, N., Gerard, C., Ehlers, S., Mollenkopf, H., Kaufmann, S., 2003. Early granuloma formation after aerosol *Mycobacterium tuberculosis* infection is regulated by neutrophils via CXCR3-signaling chemokines. Eur. J. Immunol. 33 (10), 2676–2868.

Singer, B., Kirschner, D.E., 2004. Influence of backward bifurcation on interpretation on R_0 in a model of epidemic tuberculosis with reinfection. Math. Biosci. Eng. 1 (1), 81–93.

Smolle, J., 1998. Cellular automaton simulation of tumor growth—equivocal relationships between simulation parameters and morphologic pattern features. Anal. Cell Pathol. 17, 71–82.

Smolle, J., Stettner, H., 1993. Computer simulation of tumor cell invasion by a stochastic growth model. J. Theor. Biol. 160, 63–72.

Sprent, J., 1993. Lifespans of naive, memory and effector lymphocytes. Curr. Opin. Immunol. 5, 433.

Stone, K., Mercer, R., Gehr, P., Stocksill, B., Crapo, J., 1992. Allometric relationships of cell numbers and size in the mammalian lung. Am. J. Respir. Cell Mol. Biol. 6, 235–243.

Styblo, K., 1980. Recent advances in epidemiological research in tuberculosis. Adv. Tuberc. Res. 20, 1–63.

Tufariello, J., Chan, J., Flynn, J., 2003. Latent tuberculosis: mechanisms of host and bacillus that contribute to persistent infection. The Lancet 3, 578–590.

Victor, T., Warren, R., Butt, J., Jordaan, A., Felix, J., Sirgel, F., Schaaf, H., Donald, P., Richardson, M., Cynamon, M., Van Helden, P., 1997. Genome and MIC stability in *Mycobacterium tuberculosis* and indications for continuation of use of isoniazid in multidrugresistant tuberculosis. J. Med. Microbiol. 46 (10), 847–857.

Walz, A., Kunkel, S., Strieter, R., 1996. C–x–c chemokines—an overview. In: Koch, A.E., Strieter, R.M. (Eds.), Chemokines in Disease. R.G. Landes, Austin.

Webb, S., Pollard, J., Gareth, J., 1996. Direct observation and quantification of macrophage chemoattraction to the growth factor CSF-1. J. Cell Sci. 109, 793–803.

Wigginton, J., Kirschner, D., 2001. A model to predict cell-mediated immune regulatory mechanisms during human infection with *Mycobacterium tuberculosis*. J. Immunol. 166, 1951–1967.

World Health Organization, 2001. WHO Report 2001: Global Tuberculosis Control. Technical Report, World Health Organization

Zahrt, T., 2003. Molecular mechanisms regulating persistent *Mycobacterium tuberculosis* infection. Microbes Infect. 5, 159–167.

Zhang, M., Gong, J., Lin, Y., Barnes, P., 1998. Growth of virulent and avirulent *Mycobacterium tuberculosis* in human macrophages. Infect. Immun. 66, 794–799.